

Rb adsorption on the Si(001)2×1 surface: An x-ray-standing-waves study

P. Castrucci

Università Camerino, Dipartimento di Matematica e Fisica, via Madonna delle Carceri, 62032 Camerino (Macerata), Italy

S. Lagomarsino and F. Scarinci

Istituto di Elettronica dello Stato Solido, Consiglio Nazionale delle Ricerche, via Cineto Romano 42, 00156 Roma, Italy

G. E. Franklin

Department of Physics, Harvard University, Cambridge, Massachusetts 02138

(Received 30 March 1994; revised manuscript received 11 October 1994)

The Rb adsorption site distribution on the Si(001)2×1 surface and the alkali-metal Si bond length have been determined for low (0.19 ± 0.02 ML) alkali-metal coverages using the x-ray-standing-wave fields generated by (004), (113), and (022) bulk-diffracting planes. Rb atoms have been found to adsorb preferentially at valley (V) sites and on top of the higher of the Si asymmetric dimers (T_1). The bond length was found to be 3.06 ± 0.03 Å, a few tenths of an angstrom shorter than the sum of the Rb and Si covalent radii. The rearrangement of the Si outmost layer has also been discussed.

INTRODUCTION

The structural and electronic properties of alkali-metal-silicon interfaces have recently attracted a great deal of interest. In fact, the monovalent character of alkali-metal atoms and the absence of interdiffusion or silicide formation make this interface a model system to study chemisorption, bonding, and surface metallization.^{1,2} Despite the research efforts devoted to the understanding of these heterostructures, controversial results have often been reported. Since Levine's³ pioneering work on the Cs/Si(001) interface, several authors have assumed the alkali metal to reside at the pedestal site^{2,4-7} (see Fig. 1). Conversely, a sharing between a pedestal and valley adsorption has been deduced by x-ray photoelectron diffraction^{8,9} and x-ray standing-wave (XSW) (Ref. 10) experiments at saturation coverage, while adsorption mainly at cave sites (C) have been proposed by several theoretical calculations¹¹⁻¹³ and experimentally deduced for annealed samples.^{14,10} Scanning tunneling microscope (STM) images also give some contradictory results. Hasegawa *et al.*¹⁵ reported alkali-metal adsorption on

the upper atom of the asymmetric dimer pair for very low coverages (0.02 ML) and formation of linear chains perpendicular to dimer rows for 0.05 ML. However, Effner *et al.*¹⁶ found no adsorbate order till $\frac{1}{3}$ of the saturation coverage, when small domains, showing a 2×3 reconstruction, appeared. Concerning the alkali-metal-Si bond length, values ranging between an ionic type of bonding and a covalent one have been proposed.^{1-2,17-22} The purpose of our x-ray standing-wave experiment was to investigate the Rb/Si(001) interface using as many reflections as possible, in order to discriminate among several adsorption models. Low-coverage samples, obtained by depositing the alkali metal onto the substrate held at room temperature, have been studied. To our knowledge, this is the first time that XSW experiments have been performed on as-grown low-coverage Rb/Si(001) samples, and that such alkali metal interfaces have been investigated by using three reflections.

EXPERIMENT

The experiment was carried out at the X15A beam line at the National Synchrotron Light Source at Brookhaven National Laboratory. Both preparation of the sample and the x-ray standing-wave experiment were performed in ultrahigh vacuum (base pressure 5×10^{-11} Torr).²²

The Si(001) samples were cleaned with the Shiraki-etch procedure before insertion into the chamber. By heating the Si(001) crystal to about 850 °C, we obtained sharp low-energy electron-diffraction (LEED) patterns indicating a high degree of the 2×1 surface reconstruction order. The alkali metal was evaporated from a carefully outgassed SAES dispenser onto the sample which was held at room temperature. The coverage was determined by comparing the relative intensities of the x-ray fluorescence peaks (Rb $K\alpha$ with respect to Si $K\alpha$) with those obtained on a standard sample capped with Si and previously calibrated with Rutherford backscattering. The ac-

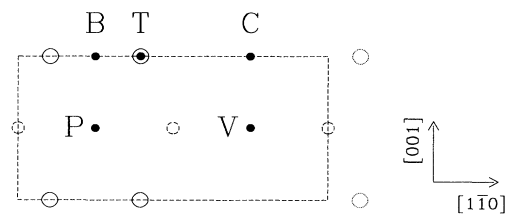


FIG. 1. Top view of the Si(001)2×1-reconstructed surface. White circle: Si outmost layer. The larger circles correspond to the first Si layer, the smaller to the second layer. The black circles refer to adsorption sites: pedestal (P), bridge (B), valley (V), cave (C), and top (T).

curacy of the measurements is better than 10%. All coverages are given in monolayers (ML), where $1 \text{ ML} = 6.78 \times 10^{14} \text{ atoms/cm}^2$, the atomic density of the $\text{Si}(001)2 \times 1$ cell. The coverage for most of the experiments was 0.19 ML.

X-RAY STANDING-WAVE ANALYSIS

The x-ray standing-wave technique measures the positions of the overlayer atoms with respect to the substrate lattice planes, by recording the adsorbate fluorescence intensity $Y(\theta)$ and the substrate reflectivity $R(\theta)$, as a function of the diffraction angle θ . $Y(\theta)$ is given by

$$Y(\theta) \propto 1 + R(\theta) + 2\sqrt{R(\theta)}F \cos[\nu(\theta) - 2\pi P], \quad (1)$$

where $\nu(\theta)$ is the phase between the incident and the diffracted wave fields.^{23,24} The two fitting parameters P and F , commonly called the coherent position and the coherent fraction, are related to the position P_i and to the probability f_i of the individual sites in the following way:²⁵

$$\tan(2\pi P) = \frac{\sum_i f_i \sin(2\pi P_i)}{\sum_i f_i \cos(2\pi P_i)} \quad (2)$$

and

$$F = f_{\text{com}} \left[\left[\sum_i f_i \sin(2\pi P_i) \right]^2 + \left[\sum_i f_i \cos(2\pi P_i) \right]^2 \right]^{1/2}, \quad (3)$$

f_{com} is a factor related to the static and dynamic (thermal variation) disorder. Its value can range between 0 and 1: the higher the disorder, the smaller the value of f_{com} . Though each P_i value is strictly related to a peculiar adsorption site, it is also affected by the bond length and by the atomic structure of the outermost substrate layers. Therefore, a complete structural description of the interface generally requires XSW measurements along several noncoplanar diffracting planes.²⁶

RESULTS AND DISCUSSION

An asymmetrically cut $\text{Si}(004)$ monochromator was employed to study both the (004) and (113) diffracting planes, while an asymmetrically cut $\text{Si}(022)$ monochromator was used to study the (022) reflection. As the monochromator change procedure generally takes some hours and the Si-alkali-metal interfaces are reactive even at a pressure of 5×10^{-11} torr, a low-coverage (0.17 ML) sample was grown to record the data coming from (022) reflection. The (004) planes are parallel to the surface, while the (113) and (022) planes form an angle of 25.14° and 45° , respectively, with the surface. The crystal reflectivity and adsorbate fluorescence curves are shown in Fig. 2(a) for both (004) and (113) reflections and in Fig. 2(b) for the (022) reflection. Table I summarizes the experimental results.

Our measured coherent fraction F values were never larger than 0.4. As this was a well-reproducible result, it clearly suggests that Rb atoms adsorb simultaneously at different sites.

In order to obtain the alkali-metal adsorption model, we followed a two-step analysis.

(1) Starting from theory and previous experiments, we made reasonable assumptions about the interface geometry and the bond lengths. In this way, we chose all the parameters and their variability ranges which are necessary to obtain a description of the adsorption process.

(2) For each reflection, we compared the experimental P and F values with the corresponding ones calculated for each set of parameters taken into account. Then we selected only those sets giving, for all the reflections, P and F values equal, within the errors, to experimental ones. In this way, we obtained a limited range of possible structural models of the interface.

STM studies have shown that the atomic structure of the $\text{Si}(001)2 \times 1$ -reconstructed surface is a mixture of a certain amount of buckled dimers, stabilized by defects, in extensive areas of oscillating dimers whose time-averaged position is the symmetric one.^{27,28} In the literature the commonly considered adsorption sites for

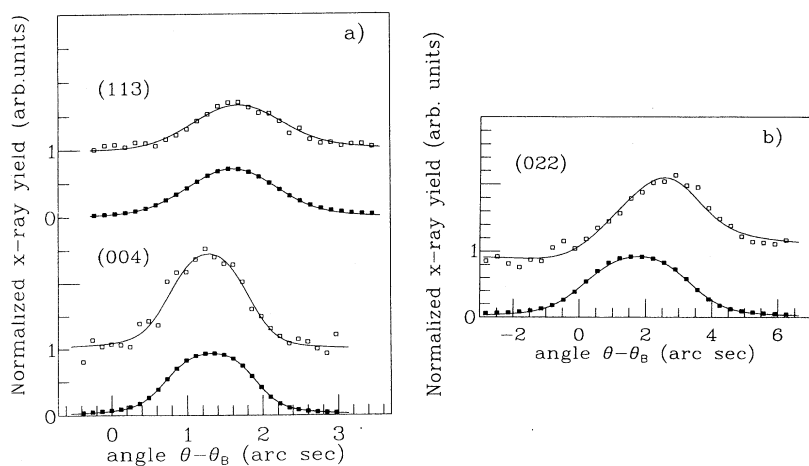


FIG. 2. X-ray standing-wave Rb measurements, related to the (004) and (113) reflections [panel (a)] and to the (022) [panel (b)]. The fluorescence yield and diffracted intensity are indicated by open and filled squares, respectively. Solid lines are theoretical fits to the experimental data.

TABLE I. Experimental results and best-fit values, as obtained from data analysis described in the text, for the coherent position P and coherent fraction F related to each (hkl) reflection.

(hkl)	Experimental results		Best-fit values		
	P	F	P	F	f_{com}
(004)	0.23 ± 0.03	0.36 ± 0.05	0.24 ± 0.02	0.37 ± 0.02	0.69 ± 0.02
(113)	0.57 ± 0.05	0.09 ± 0.05	0.53 ± 0.01	0.09 ± 0.03	0.58 ± 0.09
(022)	0.50 ± 0.05	0.38 ± 0.05	0.46 ± 0.01	0.39 ± 0.03	0.86 ± 0.01

Si(001)2×1 cell are the so-called bridge (B), pedestal (P), cave (C), valley (V) (see Fig. 1), and top (T_1 and T_2) (see Fig. 3), i.e., the site on top of the highest of the two atoms forming the asymmetric dimer. Concerning the first four (BPCV) sites, we assumed that the alkali-metal atoms adsorption at the BPCV sites symmetrize the respective dimer, while we supposed that a modification of the buckling angle may occur when the alkali-metal atoms adsorb on the top site. The hypothesis of a symmetrization of the silicon atoms induced by the adsorption at one of the BPCV sites has often been taken into account by several authors. As a consequence of the induced symmetrization of the silicon dimers, it was impossible to know, *a priori*, the actual position of the silicon atoms after alkali-metal adsorption. Therefore, we assumed the outermost silicon atoms may place at any position between two extreme arrangements of the silicon surface, i.e., the symmetric dimer model and the nonreconstructed surface. Thus we considered the silicon atom coordinates calculated by Payne²⁹ in his symmetric dimer model of the Si(001)2×1 reconstruction as starting values, and we indicated as Δz the distance, in the [001] direction, between the actual position of the silicon atoms and the position calculated by Payne [see Fig. 4(a)]. Δz was therefore assumed to range from 0.00 to 0.43 Å. Positive values refer to a displacement in the outward direction.

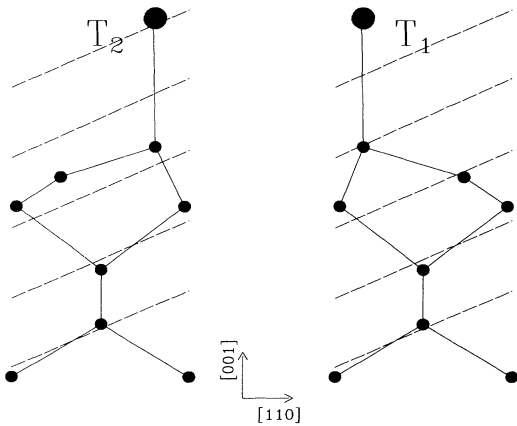


FIG. 3. Side views of the silicon surface, where the T_1 and T_2 adsorption sites for a Si(001) (1×2) domain are indicated. The (113) planes and the T_1 and T_2 different distances with respect to them are shown.

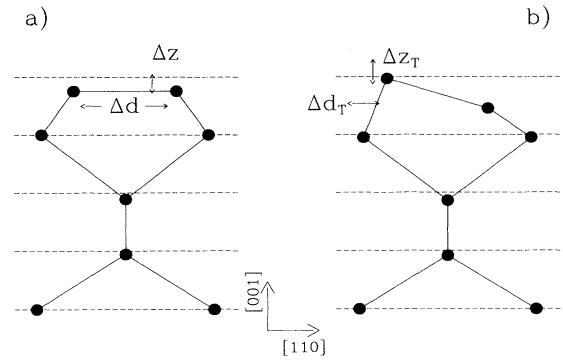


FIG. 4. (a) Side view of the symmetric dimers according to Payne's calculations (Ref. 29). The Δz and d parameters represent the allowed displacements, upon Rb adsorption, of the silicon dimer atoms out of plane and in plane, respectively. (b) Side view of the asymmetric dimers according to Northup's model (Ref. 30). Δz_T and Δd_T represent the allowed displacements, due to alkali-metal adsorption, of the highest of the two atoms forming the asymmetric dimer.

In order to account for in-plane rearrangement, we named d the relative distance along the [110] direction between the two atoms forming the dimer, and we let this distance vary from 2.23 (d value calculated by Payne²⁹) and 3.84 Å (proper distance between two bulk silicon atoms).

Concerning the adsorption at the top site, we considered only the position of the Si atom bound to the alkali metal, i.e., the highest of the two atoms forming the asymmetric dimer. In this case, we started from the Northup's³⁰ model which gives the coordinates of the Si atoms forming the asymmetric dimer. Thus we indicated as Δz_T and Δd_T the difference between the actual silicon-atom position and the one calculated by Northrup along the [001] and [110] directions respectively. In our analysis we allowed Δz_T to vary from -0.15 to 0.15 Å, and Δd_T to range from -0.30 to 0.05 Å [see Fig. 4(b)]. The positive sign of Δz_T is referred to as a displacement in the outward direction, while the positive sign of Δd_T is referred to as a displacement toward the other Si atom forming the asymmetric dimer.

Concerning the nature of the alkali-metal–Si bond, different theoretical studies point at ionic as well as covalent types of bonding. Surface-extended x-ray-adsorption fine-structure experiments, carried out on full-coverage K/Si(001) and Na/Si(001) interfaces, indicated bond lengths approximately equal to the sum of the covalent radii of the alkali metal and silicon. To our knowledge no direct measurements are, up to now, available for Rb atoms.

Therefore, we allowed the bond length (BL) between the alkali metal and the silicon atom to range from 2.65 to 3.60 Å, thus accounting for all intermediate values between an ionic type of bonding and a covalent type.

At this point, we had to determine the distribution of Rb atoms among the six sites ($BPCV$, T_1 , and T_2) taken into consideration and the values of the parameters Δz , d ,

Δz_T , Δd_T , and BL. Each set of values of these parameters and each adsorption site give different distances of the Rb atoms with respect to the diffraction planes (004), (022), and (113). As an example, in Table II we report the Rb positions with respect to the above-mentioned planes calculated for the six sites and for the following values of the parameters: $\Delta z=0$ Å, $d=2.23$ Å, $\Delta z_T=$ Å, $\Delta d_T=0$ Å, and BL=3.40 Å. This situation corresponds to the silicon-atom coordinates calculated by Payne²⁹ for the symmetric dimer model and by Northup³⁰ for the asymmetric dimer ones, and to a covalent type of bonding. In Table II the (a) and (b) superscripts indicate the two possible domains (2×1) and (1×2) allowed in the Si(001) 2×1 reconstruction. As our Si samples were cut with the surface parallel to the (001) planes within a few minutes of arc, we expect an equiprobable presence of 2×1 and 1×2 silicon surface domains. This expectation was confirmed by LEED patterns which gave equintensity spots for the two domains. It is interesting to note that, for the two domains, the distances with respect to (113) diffracting planes of the Rb atoms adsorbed at bridge and valley sites differ 0.5 times the interplanar distance. As a consequence, simultaneous adsorption on these sites gives rise to a very low coherent fraction.

In order to come to a determination of the site distribution and of the values of the parameters defined above, we carried out our analysis through a very simple algorithm made up of 12 nested loops: six for the sites occupancy, five for the parameters, and one for the f_{com} value [see Eq. (3)]. The occupancy at each site was let to vary from 0 to 1, with steps of 0.1. The range of the allowable values for each parameter has been reported above, while the value of the step was in all cases 0.01 Å. Concerning the f_{com} value, we made the following considerations: both the (004) and the (022) reflections gave a resulting coherent fraction of the order of 0.4. Therefore, we assumed that this was the minimum value that could be attributed to f_{com} , which represents the combined effect of the static and dynamic disorder. We interpreted the very low value assumed by the coherent fraction for the (113) reflection as due mainly to the simultaneous presence of the two kinds of domains [(2×1) and (1×2)]. In fact, as can be seen in Table II, Rb atoms adsorbed on bridge and valley sites experience, for the two domains, two positions which are completely out of phase with respect to

TABLE II. Expected Rb positions (in units of interplanar spacing) calculated according to Payne's (Ref. 29) symmetric dimer coordinates for bridge, pedestal, cave, and valley sites and to Northup's (Ref. 30) values for top sites. The Rb-Si bond length was assumed to be the sum of covalent radii. Superscripts (a) and (b) discriminate between the P_i calculated values for the two (2×1) domains.

	<i>B</i>	<i>P</i>	<i>C</i>	<i>V</i>	<i>T</i> ₁	<i>T</i> ₂
P_{004}	0.609	0.137	0.809	0.839	0.976	0.976
$P_{113}^{(a)}$	0.207	0.353	0.107	0.920	0.482	0.482
$P_{113}^{(b)}$	0.707	0.353	0.107	0.420	0.640	0.324
$P_{022}^{(a)}$	0.555	0.319	0.155	0.197	0.580	0.896
$P_{022}^{(b)}$	0.555	0.319	0.155	0.197	0.896	0.580

one another. Thus we let f_{com} vary between 0.4 and 1, with a step of 0.1. By using this procedure, we examined a very large number of different combinations. For each combination of site distribution and parameters values, we calculated the resulting coherent fraction F and coherent position P for the three reflections considered, and compared them with the corresponding experimental values. Only those combinations giving agreement, within errors, with experiment have been selected. In this way a limited number (a few tens) of combinations compatible with experimental results were obtained. More importantly, all these combinations are very similar to one another, yielding values reported in Table III. The spread of parameter values of these combinations gives rise to the quoted error bars. In Table I, together with the experimental results, we report the resulting P , F , and f_{com} values for the three reflections. The small error bar comes from using three reflections; in fact, with only two reflections the number of possible solutions increases enormously, with significant differences in parameter values.

From our analysis we found a multisite occupancy, where about 60% of coherent Rb atoms adsorb at valley site, 20% at T_1 , 10% at pedestal, and 10% at bridge sites. Moreover, we obtained a bond length of 3.06 ± 0.03 Å, which suggests a partly ionic interaction. A significant rearrangement of the silicon surface due to the Rb presence is also evident. In fact, the symmetric dimer atoms break their bonding and appear approximately in Si(001) 1×1 sites. Moreover, the Rb adsorption at T_1 sites induces a displacement of the upper Si atom of the asymmetric dimer pair which could be related to an increasing of the dimer angle. Figure 5 shows schematically the kind of surface rearrangement we found.

Our conclusions, suggesting the valley as the most favorable site for about 0.20-ML Rb coverage obtained by room-temperature growth, does not exclude the possibility of a pedestal-valley configuration for saturation coverage samples,⁸⁻¹⁰ due to the fact that full occupation of valley sites constitutes only 50% of the saturation coverage. Conversely, our results are in contrast with most of the theoretical calculations made for K or Na adsorption¹¹⁻¹³ and with XSW and Auger-electron diffraction (AED) results for annealed samples,^{14,10} which indicate

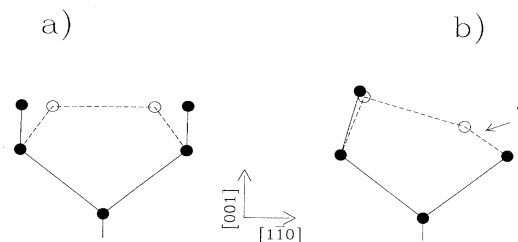


FIG. 5. Side view of the position modification of symmetric (a) and asymmetric (b) Si dimers upon rubidium adsorption. In both (a) and (b) black circles represent the actual Si positions as results from our analysis; open circles are the Si position according to Payne's (a) and Northup's (b) model.

TABLE III. Bond length BL, displacements Δz , d , Δz_T , and Δd_T , and adsorption site distributions are obtained by comparing experimental and calculated P and F .

Site distribution		Surface rearrangement	
Pedestal	0.10±0.05	BL	3.06±0.03 Å
Bridge	0.10±0.05	Δz	0.03±0.03 Å
Cave	0.00±0.05	d	3.80±0.04 Å
Valley	0.60±0.05	Δz_T	0.13±0.03 Å
Top T_1	0.20±0.05	Δd_T	-0.10±0.05 Å
Top T_2	0.00±0.05		

the cave as the most stable site. However, it must be considered that the energy difference between valley and cave configurations is generally expected to be very small,¹¹ and that Rb atoms are larger than K or Na ones; therefore a different behavior with respect to them is not surprising. On the other side, it is not possible to make a direct comparison with the annealed samples because the thermal treatment, giving energy to the system, can induce significant changes to the site distribution. Concerning the top site adsorption, it could be associated with the presence of defects on the silicon surface, which generally prevent the dimer atoms from oscillating, thus

producing the dimer asymmetry.

It must be noted that the different heights of alkali-metal atoms at the valley and top sites with respect to silicon atoms, together with the changes in the substrate outermost atom positions, allow us to draw a picture of the surface which appears to be in very good agreement with Effner *et al.*'s Si(001)/K STM images for approximately the same coverage on as-grown samples.¹⁶

In summary, x-ray standing-wave experiments have been performed for low-coverage Si(001)2×1/Rb interfaces by investigating the (004), (113), and (022) reflecting planes. The measurements suggest the valley position as the preferential adsorption site, with a small occupation at the T_1 site. Furthermore, we found a partly ionic type of bonding and a rearrangement of the Si outmost layer.

ACKNOWLEDGMENTS

We are very grateful to Dr. J. R. Patel for very helpful discussions. G.E.F. would like to acknowledge the U.S. Department of Energy for their support under Contract No. DEFG02-89ER-45399 to Harvard University and Contract No. DE-AC02-76CH00016 to the facilities of the NSLS at Brookhaven National Laboratory.

¹S. Ciraci and I. P. Batra, Phys. Rev. Lett. **56**, 877 (1986).

²C. Ciraci and I. P. Batra, Phys. Rev. B **37**, 2995 (1988).

³J. D. Levine, Surf. Sci. **34**, 90 (1973).

⁴H. Tochiyama and Y. Murata, J. Phys. Soc. Jpn. **51**, 2920 (1982).

⁵T. Aruga, H. Tochiyama, and Y. Murata, Phys. Rev. Lett. **55**, 372 (1984).

⁶R. Holtom and P. M. Gundry, Surf. Sci. **63**, 263 (1977).

⁷C. M. Wei, H. Huang, S. Y. Tong, G. S. Glander, and M. B. Webb, Phys. Rev. B **42**, 11 287 (1990).

⁸T. Abukawa and S. Kono, Phys. Rev. B **37**, 9097 (1988).

⁹T. Abukawa and S. Kono, Surf. Sci. **214**, 141 (1989).

¹⁰V. Eteläniemi, E. G. Michel, and G. Materlik, Surf. Sci. **251/252**, 483 (1991).

¹¹I. P. Batra, J. Vac. Sci. Technol. A **8**, 3425 (1990).

¹²Y. Ling, A. J. Freeman, and B. Delley, Phys. Rev. B **39**, 10 144 (1989).

¹³R. Ramirez, Phys. Rev. B **40**, 3962 (1989).

¹⁴M. C. Asensio, E. G. Michel, E. M. Oellig, and R. Miranda, Appl. Phys. Lett. **51**, 1714 (1987).

¹⁵Y. Hasegawa, I. Kamira, T. Hashizume, T. Sakurai, H. Tochiyama, M. Kubota, and Y. Murata, Phys. Rev. B **41**, 9688 (1990).

¹⁶U. A. Effner, D. Badt, J. Binder, T. Bertrams, A. Brodde, Ch. Lunau, H. Neddermeyer, and M. Handücker, Surf. Sci. **277**, 207 (1992).

¹⁷M. Tsukada, H. Ishida, and N. Shima, Phys. Rev. Lett. **53**, 376 (1984); H. Ishida, N. Shima, and M. Tsukada, Phys. Rev. B **32**, 6236 (1985).

¹⁸R. V. Kasowski and M. H. Tsai, Phys. Rev. Lett. **60**, 546 (1988).

¹⁹P. S. Bagus and I. P. Batra, Surf. Sci. **206**, L895 (1988); I. P. Batra and S. Bagus, J. Vac. Sci. Technol. A **6**, 600 (1988).

²⁰I. P. Batra, Phys. Rev. B **39**, 3919 (1989).

²¹T. Kendelewicz, P. Soukiassian, R. S. List, J. C. Woickik, P. Pianetta, I. Lindau, and W. E. Spicer, Phys. Rev. B **37**, 7115 (1988).

²²E. Vlieg, E. Fontes, and J. R. Patel, Phys. Rev. B **43**, 7185 (1990).

²³B. W. Batterman, Phys. Rev. **133**, A759 (1964).

²⁴B. W. Batterman and H. Cole, Rev. Mod. Phys. **36**, 681 (1964).

²⁵N. Hertel, G. Materlik, and J. Zegehnagen, Z. Phys. B **58**, 199 (1985).

²⁶J. A. Golovchenko, J. R. Patel, D. R. Kaplan, and M. J. Bedzyk, Phys. Rev. Lett. **49**, 560 (1982).

²⁷R. J. Hamers, R. M. Tromp, and J. E. Demuth, Phys. Rev. B **34**, 5343 (1986).

²⁸B. S. Swartzendruber, Y. W. Mo, M. B. Webb, and M. G. Lagally, J. Vac. Sci. Technol. A **7**, 2901 (1989).

²⁹M. C. Payne, N. Roberts, R. J. Needs, M. Needels, and J. D. Joannopoulos, Surf. Sci. **211**, 1 (1989).

³⁰J. E. Northrup, Phys. Rev. B **47**, 10 032 (1993).